Qiong He and Li Li*

MicroRNA-302a enhances 5-fluorouracil sensitivity in HepG2 cells by increasing AKT/ULK1-dependent autophagy-mediated apoptosis

https://doi.org/10.1515/oncologie-2023-0530
Received November 19, 2023; accepted January 21, 2024;
published online February 23, 2024

Abstract

Objectives: MicroRNA-302a (miR-302a) has been implicated in the oncogenic processes, but its role in hepatocellular carcinoma (HCC) chemoresistance and related mechanisms are still unclear. Therefore, the aim of this study was to investigate the role of miR-302a in HCC chemoresistance and elucidate its underlying mechanism.

Methods: In this study, we detected the level of miR-302a in HCC tissues (including chemoresistant and chemosensitive tissues), non-tumor tissues, liver cancer cell lines, and 5-fluorouracil (5-FU)-resistant cells (HepG2/R). Additionally, we conducted cell viability, apoptosis, and autophagy analyses as well as assessed the levels of cleaved caspase-3, cleaved caspase-9, microtubule-associated protein 1 light chain 3 beta II (LC3B-II), Akt, and UNC-51 like kinase 1 (ULK1) in HepG2 cells transfected with miR-302a mimic or inhibitor prior to 5-FU treatment. Lastly, we predicted the target of miR-302a and verified the relationship between miR-302a and Akt by luciferase reporter and functional repair assays.

Results: Our results revealed that miR-302a was down-regulated in HCC tissues ($p<0.01$), especially in chemoresistant tissues ($p<0.01$). Consistently, the miR-302a level exhibited a lower expression in HepG2/R cells compared to their parental cells ($p<0.01$). Furthermore, the 5-FU-induced apoptosis and autophagy of HepG2 cells were promoted by miR-302a over-expression and diminished by miR-302a inhibition ($p<0.01$). Target analysis revealed that miR-302a could directly target Akt. Moreover, miR-302a inhibited Akt expression and subsequently elevated ULK1 expression ($p<0.01$). Inhibition of ULK1 could abrogate the sensitization of overexpressed miR-302a to 5-FU in HepG2 cells ($p<0.01$).

Conclusions: Altogether, our results demonstrate that the down-regulation of miR-302a promotes 5-FU resistance in HCC by attenuating the Akt/ULK1 axis-dependent autophagy and apoptosis.

Keywords: liver cancer; microRNA-302a; chemoresistance; apoptosis; Akt; autophagy

Introduction

Liver cancer (LC) is ranked as the third leading cause of cancer-related mortality, contributing to an estimated annual fatality count of approximately 830,000 individuals [1, 2]. Hepatectomy and adjuvant chemotherapy are the primary treatments for LC [3]. Unfortunately, the overall survival rate has failed to meet expectations because of the development of chemoresistance and the high rate of recurrence [4]. The molecular basis of chemoresistance is still unclear and continues to be a big challenge that significantly limits the efficacy of chemotherapy. Therefore, understanding the underlying molecular mechanisms associated with chemoresistance is essential to improve the clinical outcome of LC patients.

MicroRNAs (miRNAs) are involved in regulating the biological behaviors of tumor cells, such as proliferation, invasion, apoptosis, autophagy, and chemoresistance [5–9]. Therefore, identification of the miRNA machinery that regulates LC chemoresistance will not only facilitate the understanding of LC progression but also aid in the development of potential therapeutic strategies for LC chemoresistance [10, 11]. MicroRNA-302a (miR-302a), a member of the miR-302 family (miR-302/367 cluster), inhibits the progression of various cancers, including gastric cancer, LC, and breast cancer (BC) [12–14]. Additionally, miR-302a over-expression enhances the sensitivity of multiple tumor cells to chemotherapy agents [9, 15–17]. Although miR-302a plays a regulatory role in various tumors, its effect on 5-fluorouracil (5-FU) sensitivity in LC cells remains unclear.

Autophagy is also implicated in the modulation of chemoresistance [18–23]. However, autophagy plays a dual role in the regulation of chemotherapy. On one hand, autophagy serves as a mechanism to enhance the sensitivity of cancer cells to chemotherapy, acting as a chemosensitizing agent. For instance, autophagic cell death can significantly

***Corresponding author: Li Li**, Department of Nursing, Wuhan Red Cross Hospital, Wuhan, China, E-mail: lli0325@163.com
Qiong He, Department of Gastroenterology, Wuhan Red Cross Hospital, Wuhan, China

increase the responsiveness of non-small cell lung cancer and cervical cancer cells toward chemotherapeutic agents [18, 19]. On the other hand, autophagy can have an antagonistic effect on chemotherapy-induced cell death and can reduce sensitivity toward chemotherapy [20–23]. These differences may be related to cell types, cell states, autophagy threshold, etc. Nevertheless, regulation of autophagy may be a novel strategy to overcome chemoresistance. Autophagy is regulated by multiple genes, miRNAs, and kinases, among which UNC-51 like kinase 1 (ULK1) acts as a switch for autophagy [24]. ULK1 is the substrate of the mammalian target of rapamycin (mTOR) complex 1 (mTORC1), which is accommodated by the upstream protein kinase B (PKB/Akt)/mTOR signaling [25, 26]. Interestingly, miR-302a has been documented to suppress Akt signaling while inducing cancer cell death and enhancing sensitivity toward chemotherapeutic agents [16, 27]. In the study, we identified *Akt* as a potential target gene for miR-302a using target gene prediction software. These findings suggest an intrinsic relationship between miR-302a, Akt, autophagy, and 5-FU sensitivity in LC cells. Therefore, our study aimed to explore the correlation between miR-302a, Akt, autophagy, and 5-FU sensitivity in LC cells and to provide evidence on the regulatory role of miR-302a on 5-FU chemoresistance in LC cells *via* the Akt/ULK1-dependent autophagy and apoptosis.

Materials and methods

Materials and reagents

5-FU (#F6627), 4′, 6-diamidino-2-phenylindole (DAPI) dye (#D9542), 3-methyladenine (3-MA, #M9281), and hematoxylin (#H3136) were from Sigma-Aldrich (MO, USA). ULK1 inhibitor SBI-0206965 (#HY16966) and Akt inhibitor GSK690693 (#HY10249) were from MedChemExpress (NJ, USA). Opti-minimal essential medium (Opti-MEMI) (#31985070), Dulbecco's modified Eagle's medium (DMEM) (#11965092), and fetal bovine serum (FBS, #12483020) were from Gibco (CA, USA). MiR-302a (MI0000738) mimic miR-302a-m (5′-UAAGUGCUUCCAUGUUUUGGUGA-3′), miR-302a inhibitor miR-302a-i (5′-AUUCACGAAGGUACAAAACCACU-3′), and their corresponding negative control plasmids NC-m (5′-UUGUACUACACAAAAGUACUG-3′) and NC-i (5′-UUCUCCGAACGUGUCACGUTT-3′), respectively, were synthesized by Sangon Biotech (Shanghai, China).

Patients and specimen preparation

The research protocols were approved by the Wuhan Red Cross Hospital Ethics Committee (2015-102), and were performed in accordance with the Helsinki Declaration. Written informed consent was obtained from all individuals included in this study. The present study included 37 hepatocellular carcinoma (HCC) patients, who had received pathological examinations and chemotherapy from 2015 to 2018 in the Wuhan Red Cross hospital. The clinical baseline data of the patients are listed in Table S1. Chemosensitive patients were defined as those who showed a good response to chemotherapy and had a recurrence time of >2 years (n=20), while chemoresistant patients were defined as those who responded poorly to the previous chemotherapy and relapsed in ≤1 year (n=17). The HCC tissues and matched adjacent noncancerous tissues of the patients were harvested during surgical resection prior to 5-FU + cisplatin (FP) chemotherapy. All the clinical samples were processed for subsequent pathological examination and real-time polymerase chain reaction (PCR) analysis.

Cell culture and transfection

Transformed human liver epithelial-3 (THLE-3) cells and LC cell lines (HCC-LM3, SMMC-7721, Bel-7402, and HepG2) were purchased from SUNNCELL Cell Bank (Wuhan, China) and were authenticated by STR profiling. Mouse primary hepatocytes were isolated as described previously [27]. All the cells were grown in DMEM supplemented with 100 U/mL penicillin/0.1 mg/mL streptomycin (#15140148, Gibco), and 10 % FBS at 37 °C in a 5 % CO_2 incubator. 5-FU-resistant cells (HepG2/R) were established by treating HepG2 cells with increasing concentrations of 5-FU over 2 years (evidence for the successful construction of HepG2/R was shown in Figure S1). To ensure the absence of residual 5-FU inference, HepG2/R cells were cultured without 5-FU stimulation for 2 weeks before experiments. For miRNA transfection, miR-302a-m, miR-302a-i, NC-m, or NC-i were transfected into HepG2 cells by Lipo Transfection Reagent (#KGD031, Keygen, Nanjing, China) according to the manufacturer's protocol as described previously [9, 15–17].

In situ hybridization (ISH)

The paraffin-embedded HCC tissues were sectioned, deparaffinized thrice in xylene, and rehydrated through an ethanol series. Thereafter, the sections were incubated with the miR-302a probe (40 nM double-DIG LNA™ microRNA probe, Exiqon, Denmark). The sections were counterstained with hematoxylin and observed under an Olympus light microscope (Tokyo, Japan). Positive staining of ISH from five nonoverlapping fields in each section was statistically analyzed by the IHC Profiler of the Image J software (v1.57, NIH, Maryland, MD). The IHC Profiler used the average staining intensity and positive staining area as the ISH measurement indicators and automatically gave a score, <1 indicated negative, >1 indicated positive, and higher scores indicated stronger positive expression.

Real-time PCR

The total RNA from HCC tissues, hepatocytes, or cultured LC cells was extracted using the RNA isolation kit (Qiagen RNAeasy Mini Kit, Qiagen, NV, Netherlands). The miR-302a levels were quantified by performing real-time PCR on Mx3000P qPCR Systems (Agilent, CA, USA) using the MicroRNAs qPCR Kit (#B532461, Sangon Biotech). The miRNA primers were purchased from GeneCopoeia (Guangzhou, China). The relative mRNA levels were normalized to U6 snRNA (U6).

Cell viability assay

The viability of HepG2 cells was measured using a cell counting kit (CCK-8; #CK04, Dojindo, Tokyo, Japan). Briefly, HepG2 cells transfected with miR-302a-m or miR-302a-i were cultured in 96-well plates (10^3 cells/well) and then rendered quiescent by culturing in 0.2 % FBS/DMEM for 24 h. The cells were then pretreated with or without 3-MA (5 mM), SBI-0206965 (10 μM), or GSK690693 (1 μM) for 30 min and then treated with or without 5-FU (10, 50, 100 μM) for 24 h. Thereafter, the cells were incubated with CCK-8 solution for 4 h at 37 °C and the absorbance was determined at 490 nm wavelength using a spectrophotometer (SPECTRA MAX190, Sunnyvale, CA).

TUNEL staining

Cell apoptosis was determined using the TUNEL detection kit (#G3250, Promega, Madison, WI, USA). Briefly, HepG2 cells were permeabilized with 0.1 % Triton X-100 for 5 min and then stained with TUNEL reagent at 37 °C for 1 h. The nuclei were counterstained with DAPI. Lastly, the cells were observed under the FV1000 confocal microscope (Olympus), and the percentage of apoptotic ($TUNEL^+$) cells was presented as $TUNEL^+$ cells/field.

Western blotting

The HepG2 cells were lysed using radio-immunoprecipitation assay (RIPA) buffer (#P0013C, Beyotime, Shanghai, China) containing a protease inhibitor cocktail (#04693116001, Roche, IN, USA). The contents of the protein extract were assessed using the BCA Kit (#P0010, Beyotime). The protein samples were then transferred onto polyvinylidene difluoride membranes (Millipore, MA, USA) using an electrophoretic transfer system (V8, Tanon, Shanghai, China). The membranes were then incubated with antibodies against Akt (1:1,000; #4685), cleaved caspase-3 (1:1,000; #9664), microtubule-associated protein 1 light chain 3 beta (LC3B)-I/II (1:500; #2775), cleaved caspase-9 (1:500; #9501), ULK1 (1:500; #8054), p62 (1:1,000; #23214) (Cell signaling Technology, Billerica, MA, USA), and β-actin (1:1,500; #sc-47778, Santa Cruz, CA, USA). Thereafter, the membranes were incubated with Horseradish peroxidase (HRP)-labeled goat anti-rabbit (1:4,000; #SA00001-2) or goat anti-mouse (1:4,000; #SA00001-1) antibodies (Proteintech, Rosemont, IL, USA) and observed under the SH-Advance 523 chemiluminescence imaging system (Shenhua Science Technology Inc., Shanghai, China). The densitometry of bands was quantified using the Image J software.

Identification of autophagy maker

The GFP-LC3 plasmids (Cyagen Biosciences Inc., Suzhou, China) were diluted in serum free-Opti-MEMI and transfected transiently into HepG2 cells. After 6 h of incubation, the cells were transferred and re-cultured in 10 % FBS/DMEM for 24 h and subjected to various treatments based on experimental design. The GFP immunofluorescence was observed under a laser-scanning confocal microscope (LSM 710, Carl Zeiss, Munich, Germany). The average number of GFP-LC3 *puncta* was assessed by counting >40 cells in five random fields per group.

Luciferase reporter assay

We utilized TargetScan 8.0 software (https://www.targetscan.org/vert_80/) to identify Akt as a prospective molecular target for miR-302a. The binding of miR-302a to Akt was determined by luciferase reporter assay. The 3′-untranslated region (3′-UTR) of human Akt was generated from the HepG2 genomic DNA and subcloned into the pmirGLO reporter vector (Promega), designated wild-type Akt. Meanwhile, the mutant 3′-UTR of Akt was produced by replacing 5 bp from the predicted seed region of miR-302a and inserting it into the pmirGLO reporter vector, designated mutant Akt. Then the cells were transfected with wild-type or mutant luciferase reporters as well as miR-302a-m or miR-302a-i, and their luciferase activities was calculated by the Dual-Luciferase Reporter Assay System (Promega).

Statistical analysis

All data were expressed as the mean ± standard deviation. Statistical analysis between two groups was performed by unpaired two-tailed Student's t-test and between multiple groups was performed by one-way analysis of variance using the SPSS software (v18.0; IBM, Chicago, IL, USA). The Pearson correlation test was used for regression analysis. The p-value <0.05 was considered statistically significant.

Results

MiR-302a levels are correlated with 5-FU-resistance in HCC

To examine the role of miR-302a in HCC, we initially used ISH to observe the expression of miR-302a in HCC tissues. ISH images showed that miR-302a was down-regulated in HCC tissues compared to the adjacent non-tumor tissues (Figure 1A and B, $p<0.01$), which was further confirmed by real-time PCR analysis (Figure 1C, $p<0.01$). Consistently, miR-302a levels were low in cultured LC cell lines (Figure 1D, $p<0.01$), especially in HepG2 cells, wherein it was only 0.4-fold of that in the cultured normal liver cells. Chemoresistance is one of the major contributors to poor prognosis in HCC patients [6]. Therefore, we collected HCC tissues that had been surgically resected before the receipt of FP chemotherapy. The HCC tissues were classified into chemosensitive and chemoresistant tissues, according to the response of patients to FP chemotherapy, and their miR-302a levels were detected using ISH and real-time PCR. The results revealed that compared to the chemosensitive HCC tissues, miR-302a levels in the chemoresistant HCC tissues were significantly decreased (Figure 1E–G, $p<0.01$). Similarly, we found that miR-302a levels were significantly decreased in the 5-FU-resistant HepG2/R cells, with approximately 0.5-fold expression level of that of the parent HepG2 cells (Figure 1H, $p<0.01$). These findings suggest that 5-FU chemoresistance is associated with the down-regulation of miR-302a expression in HCC cells.

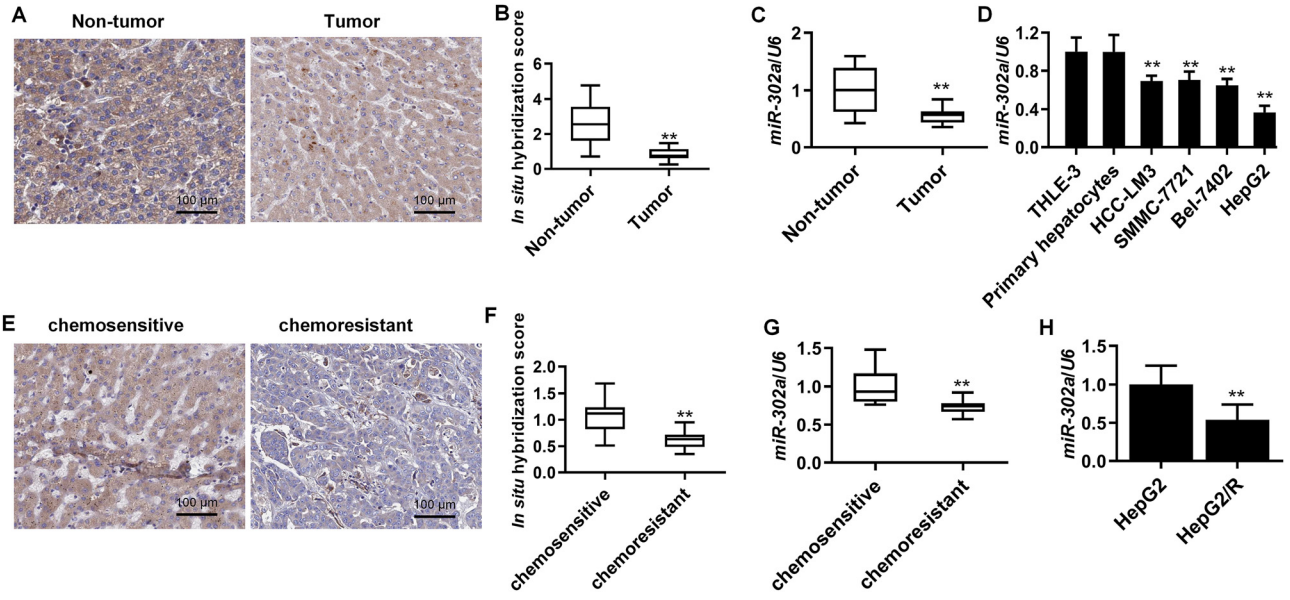

Figure 1: Decreased miR-302a levels correlate with 5-FU chemoresistance in HCC. (A–C) The levels of miR-302a in HCC tissues (n=10) and adjacent non-tumor tissues (n=10) were determined by ISH (A, B) and real-time PCR (C). $^{**}p<0.01$ vs. non-tumor. (D) Real-time PCR analysis of miR-302a levels in THLE-3, primary hepatocytes, and 4 LC cell lines. $^{**}p<0.01$ vs. THLE-3 cells, n=6. (E–G) ISH (E, F) and real-time PCR (G) analysis of miR-302a levels in chemosensitive (n=20) or chemoresistant (n=17) HCC tissues. $^{**}p<0.01$ vs. chemoresistant. (H) Real-time PCR analysis of miR-302a levels in 5-FU-resistant HepG2/R cells and parent HepG2 cells. $^{**}p<0.01$ vs. HepG2 cells, n=6.

MiR-302a inhibition decreases 5-FU sensitivity in HepG2 cells

To elucidate the effects of miR-302a on 5-FU chemosensitivity, we transfected HepG2 cells with miR-302a-m, miR-302a-i (Figure S2) in response to 5-FU treatment. As shown in Figure 2A and B, HepG2 cell viability was not significantly altered after miR-302a over-expression or inhibition under basal conditions (without 5-FU treatment). However, 5-FU decreased the viability of HepG2 cells, which was enhanced by miR-302a up-regulation but diminished by miR-302 inhibition (Figure 2A and B, $p<0.01$). These results were further confirmed by TUNEL staining, which revealed that the number of TUNEL$^+$ HepG2 cells was significantly increased in the miR-302a-m+5-FU group but significantly decreased in the miR-302a-i+5-FU group, indicating an increase in 5-FU-induced apoptosis in the miR-302a-m-transfected cells (Figure 2C and D, $p<0.01$). Additionally, the over-expression of miR-302a augmented 5-FU susceptibility in other HCC cells (Figure S3). To elucidate the regulatory role of miR-302a in 5-FU-associated HepG2 cell death, we determined the level of caspase cleavage. The results revealed that 5-FU elevated the levels of caspase-3 and caspase-9 cleavage (Figure 3E–H, $p<0.01$). Moreover, the levels of caspase-3 and caspase-9 cleavage were not significantly altered by miR-302a up-regulation and down-regulation under basal conditions but were promoted by miR-302a over-expression and reduced by miR-302a inhibition in response to 5-FU (Figure 3E–H, $p<0.01$). These results indicate that miR-302a over-expression enhanced the 5-FU sensitivity in HepG2 cells.

MiR-302a inhibition decreases 5-FU chemosensitivity by suppressing autophagy in HepG2 cells

To determine the role of autophagy in 5-FU-mediated HepG2 cell death, we examined the autophagic evidence. 5-FU treatment exhibited a concentration-dependent accumulation of GFP-LC3 *puncta* compared with the control untreated HepG2 cells (Figure 3A and B, $p<0.01$). The CCK-8 assay showed that pretreatment with an autophagy inhibitor 3-MA significantly inhibited 5-FU-induced cell death of HepG2 cells (Figure 3C, $p<0.01$), suggesting that 5-FU-induced HepG2 apoptosis might be associated with autophagy activation. Thereafter, we determined whether autophagy is involved in 5-FU chemoresistance in LC cells by incubating HepG2 and HepG2/R cells with increasing concentrations of 5-FU. The results revealed that the level of LC3B-II increased with increasing concentrations of 5-FU in both HepG2 and HepG2/R cells ($p<0.01$). Interestingly, the increase in the levels of

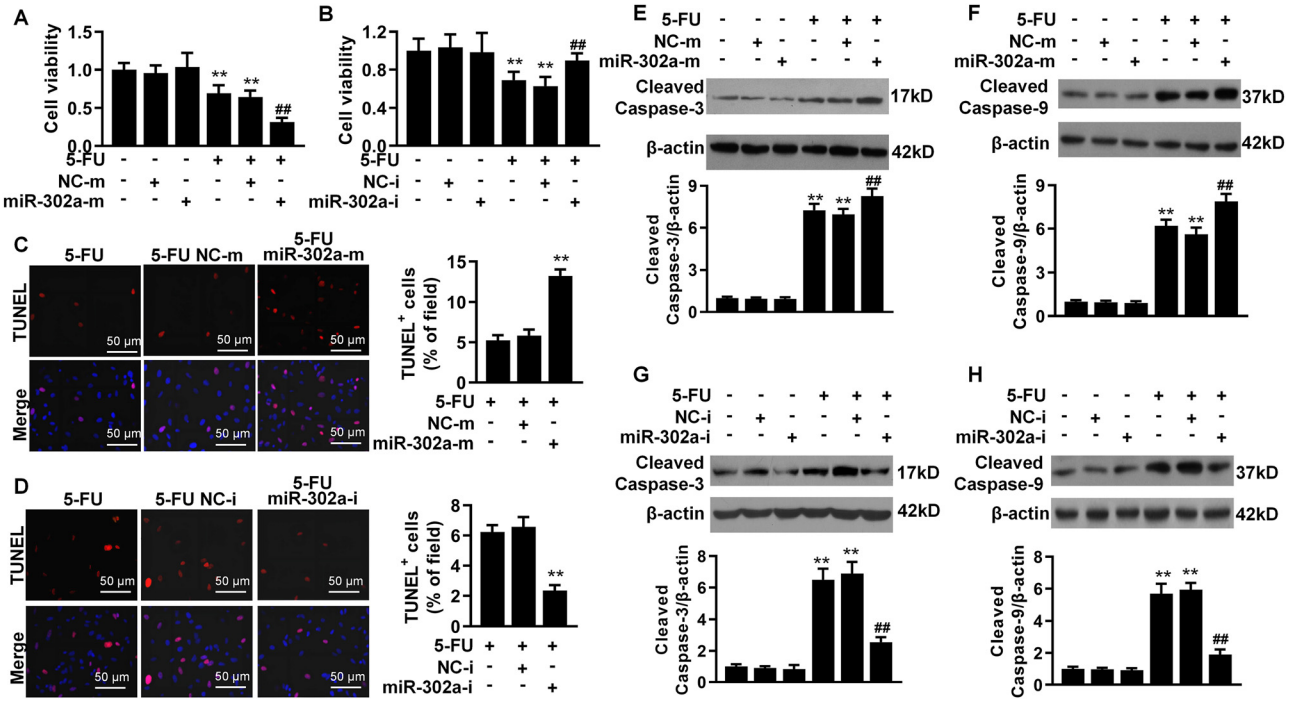

Figure 2: MiR-302a increases 5-FU sensitivity in HepG2 cells. (A, B) Statistical analysis on the effects of miR-302a-m (A) or miR-302a-i (B) transfection on the cell viability of 5-FU-treated (100 μM) HepG2 cells. **p<0.01 vs. control, $^{\#\#}$p<0.01 vs. 5-FU, n=6. (C, D) TUNEL examination and statistical analysis on the effects of miR-302a-m (C) or miR-302a-i (D) transfection on the apoptosis of 5-FU-treated (100 μM) HepG2 cells. **p<0.01 vs. 5-FU, n=6. (E–H) Western blot analysis and statistical analysis on the levels of caspase-3 (E, G) and caspase-9 (F, H) cleavage in 5-FU-treated (100 μM) HepG2 cells. **p<0.01 vs. control, $^{\#\#}$p<0.01 vs. 5-FU, n=6.

autophagy marker was more pronounced in HepG2 cells, although 5-FU led to a mild increase in LC3B-II in 5-FU-resistant HepG2/R cells (Figure 3D). Furthermore, 5-FU significantly increased the levels of miR-302a in HepG cells but not in HepG/R cells (p<0.01), even the significant differences could be only observed between 0 and 100 μM in HepG2/R cells (Figure 3E). Additionally, regression analysis revealed a positive correlation between miR-302a levels and LC3B-II expression in both HepG2 and HepG2/R cells (Figure 3F). The 5-FU-induced increase in GFP-LC3 *puncta* was significantly promoted by miR-302a over-expression and reduced by miR-302a inhibition (Figure 3G and H, p<0.01). In addition, miR-302a over-expression up-regulated LC3B-II expression and down-regulated p62 expression under 5-FU stimulation (Figure 3I and J, p<0.01). Interestingly, miR-302 expression in HepG2 cells remains unaffected by the presence of 3-MA (Figure S4). These findings suggest that miR-302a is involved in 5-FU-induced autophagy. Furthermore, pharmacological inhibition of autophagy with 3-MA reversed the effect of miR-302a on the 5-FU-induced decrease in cell viability (Figure 3K, p<0.01). Altogether, these results suggest that autophagy contributes to the enhanced effects of miR-302a on 5-FU sensitivity in LC cells.

MiR-302a targets Akt to promote autophagy-associated HepG2 cell death

To determine how miR-302a mediates autophagy in HepG2 cells, we used the TargetScan software 8.0 (https://www.targetscan.org/vert_80/) to predict the molecular targets of miR-302a. The results revealed that miR-302a might directly target Akt, a key upstream regulator of ULK1 that is involved in autophagy initiation [24, 25, 28]. Moreover, the results revealed that the miR-302a-binding site in the Akt 3′UTR (7-bp fragment) was conserved in humans and mice (Figure 4A), indicating a good conservative character. Furthermore, the results of luciferase reporter analysis revealed the luciferase activity of Akt 3′UTR decreased significantly in the miR-302a-overexpressing HepG2 cells and decreased in the miR-302a-inhibited cells (p<0.01); however, the luciferase activity of the mutant Akt 3′UTR did not alter with miR-302a over-expression or down-regulation (Figure 4B). Consistently, Akt protein expression in HepG2 cells decreased with miR-302a up-regulation and increased with miR-302a down-regulation (Figure 4C and D, p<0.01). However, ULK1 expression showed an opposing trend in HepG2 cells (Figure 4C and D, p<0.01), indicating that Akt is

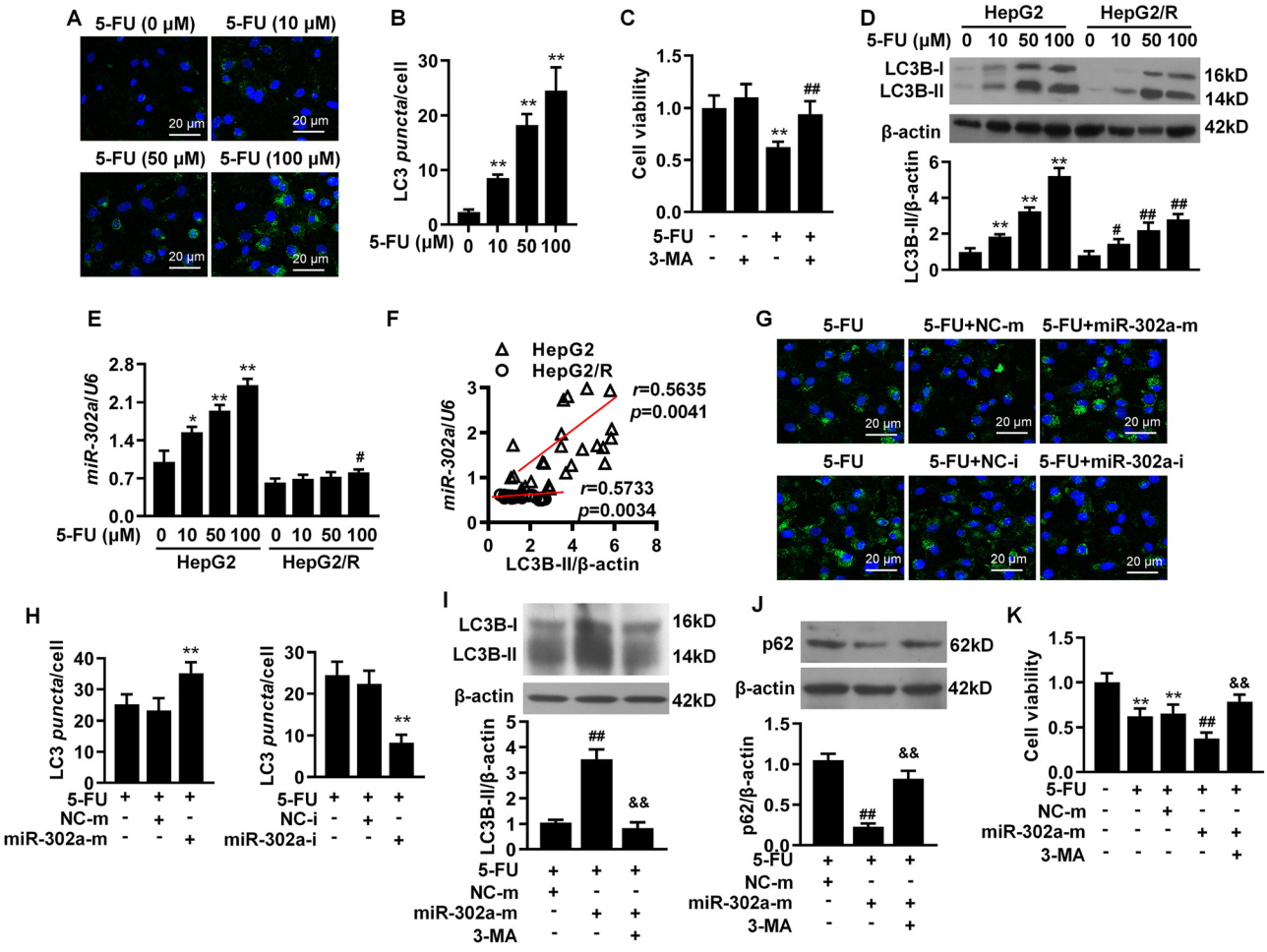

Figure 3: MiR-302a increases 5-FU sensitivity in HepG2 via autophagy. (A, B) GFP-LC3 fluorescent probe detection (A) and statistical analysis (B) on the effects of 5-FU treatment on the formation of LC3-positive *puncta* in HepG2 cells. LC3-positive *puncta* are shown from at least 40 cells from five random fields. **p<0.01 vs. control (0 μM), n=6. (C) Cell viability analysis of 3-MA-pretreated (5 μM) and 5-FU-treated (100 μM) HepG2 cells, **p<0.01 vs. untreated control, ##p<0.01 vs. 5-FU, n=6. (D, E) Levels of LC3B-I/II (D) and miR-302a (E) in 5-FU-treated (10, 50, or 100 μM) HepG2 and HepG2/R cells. *p<0.05, **p<0.01 vs. untreated HepG2 cells, #p<0.05 vs. untreated HepG2/R cells, n=6. (F) Correlation between miR-302a levels and LC3B-II expression. (G, H) GFP-LC3 fluorescent probe detection (G) and statistical analysis (H) on the effects of miR-302a-m or miR-302a-i on the formation of LC3-positive *puncta* in 5-FU-treated (100 μM) HepG2 cells. **p<0.01 vs. 5-FU, n=6. (I–K) Examination of LC3B-I/II expression (I), p62 expression (J), and cell viability (K) of miR-302a-m-transfected HepG2 cells pretreated with or without 3-MA for 30 min, and treated with 5-FU (100 μM). **p<0.01 vs. untreated HepG2 cells, ##p<0.01 vs. 5-FU+NC-m, &&p<0.01 vs. 5-FU+miR-302a-m, n=6.

a negative regulator of ULK1 [23, 24]. Considering that ULK1 has been reported to be involved in autophagy-dependent processes [23, 29, 30], we investigated whether miR-302a promotes cell death in HepG2 cells via ULK1-mediated autophagy. As shown in Figure 4E, compared with the 5-FU+NC-m group, miR-302a over-expression significantly enhanced the 5-FU-induced increase in LC3B-II levels by approximately 4.5-folds (p<0.01), which was attenuated by the ULK1 inhibitor SBI-0206965 (p<0.01). In addition, SBI-0206965 also reversed the miR-302a overexpression-induced reduction in p62 expression under 5-FU stimulation (Figure 4F, p<0.01). Moreover, SBI-0206965 significantly inhibited the enhanced activity of miR-302a on 5-FU-induced HepG2 cell death, as evidenced by the CCK-8 assay and TUNEL staining (Figure 4G–I, p<0.01). The effect of Akt1 inhibitor GSK69063 on cell viability was consistent with those of miR-302a over-expression (Figure 4G, p<0.01). Additionally, the sensitivity of miR-302a-over-expressing HepG2/R cells to 5-FU was found to be comparable to that of the parental HepG2 cells (Figure S1). Altogether, these results indicate that miR-302a enhanced 5-FU chemosensitivity by promoting Akt/ULK1-dependent autophagy in LC cells.

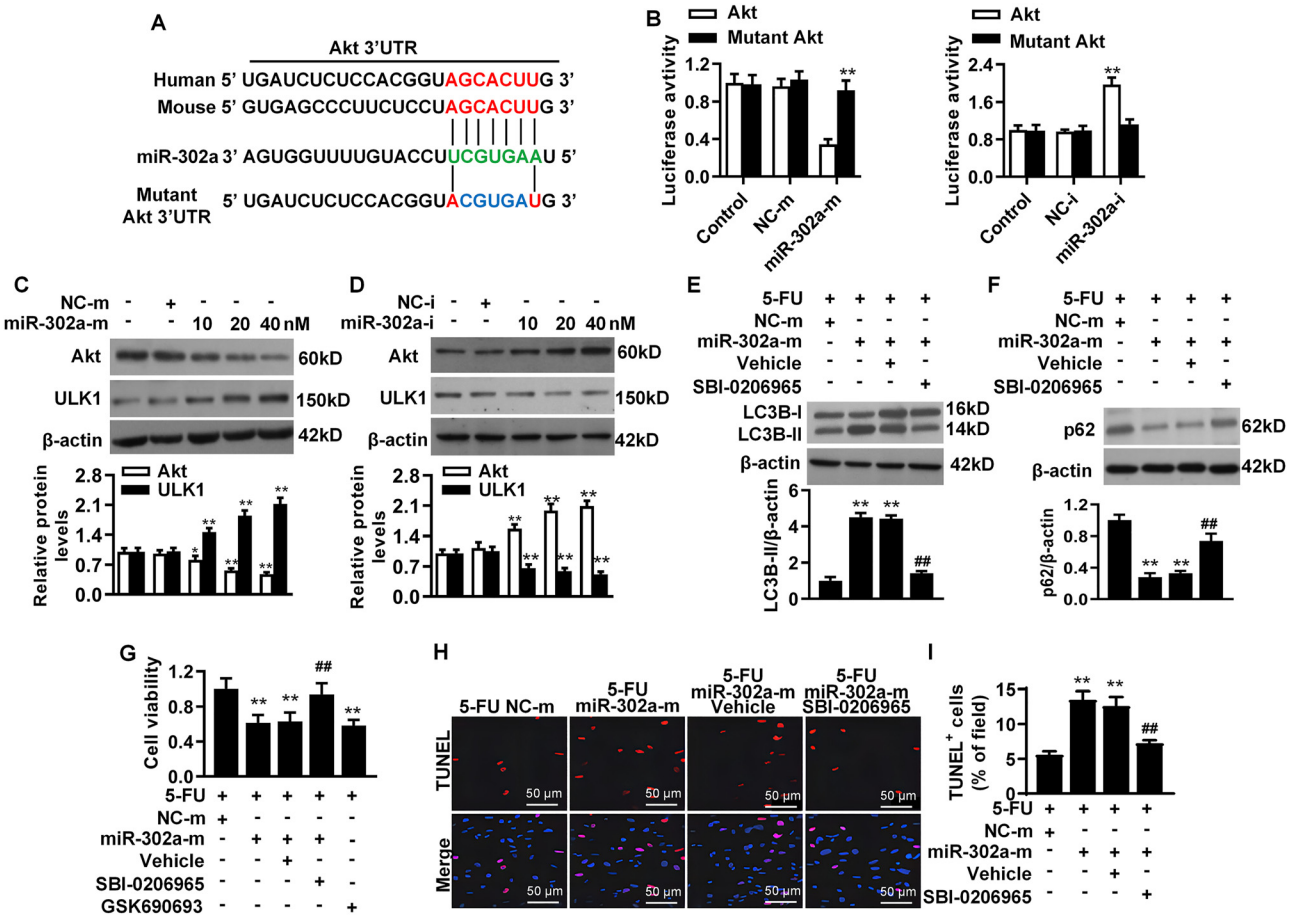

Figure 4: MiR-302a negatively regulates Akt expression and promotes autophagic death. (A) The 3′UTR of Akt was predicted as the target of miR-302a. The complementary sequences are highlighted in red and green, while the mutated sequences are highlighted in blue. (B) HepG2 cells were co-transfected with wild-type or mutant Akt 3′UTR luciferase reporter and miR-302a-m or miR-302a-i and the luciferase reporter activity was assessed. **p<0.01 vs. control, n=6. (C, D) Western blot analysis and statistical analysis of Akt (C) and ULK1 (D) protein levels in HepG2 cells transfected with increasing concentrations of miR-302a-m (C) or miR-302a-i (D) for 48 h. *p<0.05, **p<0.01 vs. control, n=6. (E–G) Examination of LC3B-I/II levels (E), p62 levels (F), and cell viability (G) of miR-302a-m-transfected HepG2 cells pretreated with SBI-0206965 (10 μM) or GSK690693 (1 μM) for 30 min and treated with or without 5-FU for 24 h. **p<0.01 vs. 5-FU+NC-m, $^{\#\#}$p<0.01 vs. 5-FU+miR-302a-m, n=6. (H, I) TUNEL staining of miR-302a-m-transfected HepG2 cells pretreated with SBI-0206965 (10 μM) or GSK690693 (1 μM) for 30 min and treated with or without 5-FU for 24 h (H) and TUNEL^{+} cell quantitation (I). **p<0.01 vs. 5-FU, $^{\#\#}$p<0.01 vs. 5-FU+miR-302a-m, n=6.

Discussion

5-FU is the most commonly used anti-cancer chemotherapeutic agents for various solid tumors, including HCC [31]. Several patients with solid tumors are initially sensitive to 5-FU but ultimately acquire chemoresistance through continuous drug administration [32], which may be attributed to changes in gene expressions and/or signaling pathways by continuous 5-FU administration. In this study, we showed that miR-302a may be an important regulator of 5-FU resistance and Akt/ULK1-dependent autophagy in LC cells. MiR-302a levels were significantly decreased in chemoresistant HCC tissues as well as 5-FU-resistant LC cells. Additionally, overexpression of miR-302a augmented the sensitivity of HepG2 cells to 5-FU treatment, while inhibition of miR-302a diminished this sensitivity. Furthermore, inhibition of miR-302a enhanced 5-FU resistance by suppressing the Akt/ULK1-mediated autophagy and subsequently inhibiting HepG2 cell apoptosis. These findings suggest that targeting miR-302a/Akt/ULK1 axis is a potential strategy for treating 5-FU resistance in HCC patients. Increasing evidence suggests that miRNAs mediate cancer cell survival and are potential regulators of chemoresistance [33]. The roles of multiple microRNAs, including miR-375, miR-205-5p, and miR-141, have been well-documented in 5-FU chemoresistance in HCC [8, 34]. For example, miR-375 levels were

found to be markedly higher in HCC tissues compared to the adjacent tissue, and its down-regulation was associated with the inhibition of 5-FU-induced cell apoptosis [8]. MiR-141 can serve as a potential 5-FU chemoresistance-reversal agent in HCC by inhibiting the antioxidant pathway [34, 35]. MiR-302a belongs to the miR-302/367 cluster, which overlaps with the La-related protein (LARP) genes, involved in RNA processing and folding [36]. This cluster has been well-characterized as a key regulator of cell proliferation and apoptosis [37]. With regards to tumor cells, the miR-302/367 cluster is suggested to be associated with increased chemosensitivity *via* the regulation of different target genes and signaling pathways [9, 15–17]. As for BC, miR-302a/b/c/d up-regulation targeted MAP/ERK kinase 1 (MEKK1) and BC resistance protein (BCRP) and increased chemosensitivity of adriamycin and mitoxantrone [15, 38]. Herein, we demonstrated that miR-302a expression was decreased in HepG2 cells and sensitized cells to 5-FU treatment, suggesting that miR-302a may function as a cancer suppressor gene in LC, consistent with some previous reports [9, 15–17, 38, 39].

Experimental and clinical investigations have shown that cell survival is critically associated with autophagic activity [18–20]; however, the mechanisms underlying this interplay are still poorly understood. Our results showed that autophagy was significantly induced by 5-FU in HepG2 cells but not in 5-FU-resistant cells. Previous studies found that the administration of 5-FU induces autophagic responses in various cancer cells, including LC cells, gastric cancer cells, and cervical cancer cells [19–22, 39]. It is worth noting that the role of autophagy in mediating cancer cell fate is inconsistent, which likely functions as a pro-survival or pro-apoptotic regulator [40]. Autophagy-mediated cell death is the predominant mechanism in response to chemotherapy [18, 19, 39]. On the other hand, autophagy may enhance tumor adaptation to stress, resulting in resistance to cell death and chemotherapy [20–23]. Therefore, maintaining a precise level of autophagic activity in specific cell types may represent a more efficacious strategy for mitigating the development of chemoresistance. Our data revealed that 5-FU-induced autophagy functions as a pro-apoptotic mechanism since the inhibition of autophagy inhibited the effects of 5-FU on HepG2 cell viability, consistent with the results of previous reports [18, 19, 39]. Moreover, the 5-FU-induced autophagy of LC cells was promoted by miR-302a over-expression and attenuated by miR-302a inhibition. These alterations provide a possible explanation for why miR-302a increases the chemosensitivity of 5-FU in LC cells.

We subsequently explored the underlying mechanisms associated with miR-302a-induced increase in LC cell autophagy using the TargetScan software, which revealed that miR-302a can directly target Akt, which is involved in autophagy initiation. Akt 3′UTR luciferase activity and protein expression were inhibited by miR-302a over-expression and increased by miR-302a inhibition. Growing evidence indicated that mTOR, a major downstream effector of Akt, exerts a critical role in regulating autophagy [23, 24, 41]. Inhibition of mTOR followed by increased ULK1 activity is critical for facilitating autophagy development [41]. Therefore, the down-regulation of Akt expression has been widely acknowledged as a reliable indicator for autophagy initiation. In this study, the miR-302a-induced inhibition of Akt was found to be accompanied by an up-regulation in ULK1 expression, providing further evidence for the involvement of miR-302a-mediated regulation of Akt levels in autophagy. Although the antineoplastic role of miR-302a may be associated with its inhibitory effects on Akt-dependent cell proliferation, our results demonstrated that ULK1 inhibitor could reverse the effects of miR-302a, suggesting that miR-302a increases chemosensitivity, at least partially, through the activation of Akt/ULK1-dependent autophagy.

Conclusions

We identified certain limitations in our study. For instance, it may be possible that miR-302a is involved in strengthening the 5-FU sensitivity of HCC cells *via* other targets or signaling pathways. Additionally, it remains unclear whether miR-302a also influences the sensitivity of other chemotherapy agents. Therefore, further research needs to be conducted on these aspects in the future. Our current findings strongly suggest that the inhibition of miR-302a in chemoresistant HCC tissues or cells may contribute to the development of chemoresistance. In contrast, miR-302a over-expression promoted 5-FU-induced autophagy and apoptosis of LC cells via the down-regulation of Akt. Therefore, the findings of our study unveiled the role of miR-302a in increasing the chemosensitivity of LC cells toward 5-FU treatment and provided a novel therapeutic strategy for LC treatment.

Research ethics: The research protocols were approved by the Wuhan Red Cross Hospital Ethics Committee (2015-102) and was performed in accordance with the Helsinki Declaration.
Informed consent: Written informed consent was obtained from all individuals included in this study.
Author contributions: All authors (Qiong He and Li Li) participated in the design of the protocol, the collection and

analysis of the data, and the writing and editing of the manuscript. All authors have accepted responsibility for the entire content of this manuscript and approved its submission.

Competing interests: The authors declare no conflict of interest.

Research funding: None declared.

Data availability: The raw data can be obtained on request from the corresponding author.

References

1. Xia C, Dong X, Li H, Cao M, Sun D, He S, et al. Cancer statistics in China and United States, 2022: profiles, trends, and determinants. Chin Med J 2022;135:584–90.
2. Sung H, Ferlay J, Siegel RL, Laversanne M, Soerjomataram I, Jemal A, et al. Global cancer statistics 2020: GLOBOCAN estimates of incidence and mortality worldwide for 36 cancers in 185 countries. CA Cancer J Clin 2021;71:209–49.
3. Brown ZJ, Tsilimigras DI, Ruff SM, Mohseni A, Kamel IR, Cloyd JM, et al. Management of hepatocellular carcinoma: a review. JAMA Surg 2023; 158:410–20.
4. Huang PS, Wang LY, Wang YW, Tsai MM, Lin TK, Liao CJ, et al. Evaluation and application of drug resistance by biomarkers in the clinical treatment of liver cancer. Cells 2023;12:869.
5. Chakrabortty A, Patton DJ, Smith BF, Agarwal P. miRNAs: potential as biomarkers and therapeutic targets for cancer. Genes 2023;14:1375.
6. Marjaneh RM, Khazaei M, Ferns GA, Avan A, Aghaee-Bakhtiari SH. The role of microRNAs in 5-FU resistance of colorectal cancer: possible mechanisms. J Cell Physiol 2019;234:2306–16.
7. Hashemi M, Rashidi M, Hushmandi K, Ten Hagen TLM, Salimimoghadam S, Taheriazam A, et al. HMGA2 regulation by miRNAs in cancer: affecting cancer hallmarks and therapy response. Pharmacol Res 2023;190:106732.
8. Dai HT, Wang ST, Chen B, Tang KY, Li N, Wen CY, et al. microRNA-375 inhibits the malignant behaviors of hepatic carcinoma cells by targeting NCAPG2. Neoplasma 2022;69:16–27.
9. Liu L, Lian J, Zhang H, Tian H, Liang M, Yin M, et al. MicroRNA-302a sensitizes testicular embryonal carcinoma cells to cisplatin-induced cell death. J Cell Physiol 2013;228:2294–304.
10. Budi HS, Younus LA, Lafta MH, Parveen S, Mohammad HJ, Al-Qaim ZH, et al. The role of miR-128 in cancer development, prevention, drug resistance, and immunotherapy. Front Oncol 2023;12:1067974.
11. Fang Y, Zhang X, Huang H, Zeng Z. The interplay between noncoding RNAs and drug resistance in hepatocellular carcinoma: the big impact of little things. J Transl Med 2023;21:369.
12. Ma G, Li Q, Dai W, Yang X, Sang A. Prognostic implications of miR-302a/b/c/d in human gastric cancer. Pathol Oncol Res 2017;23:899–905.
13. Wang M, Lv G, Jiang C, Xie S, Wang G. miR-302a inhibits human HepG2 and SMMC-7721 cells proliferation and promotes apoptosis by targeting MAP3K2 and PBX3. Sci Rep 2019;9:2032.
14. Li Z, Duan Y, Yan S, Zhang Y, Wu Y. The miR-302/367 cluster: aging, inflammation, and cancer. Cell Biochem Funct 2023;41:752–66.
15. Zhao L, Wang Y, Jiang L, He M, Bai X, Yu L, et al. MiR-302a/b/c/d cooperatively sensitizes breast cancer cells to adriamycin via suppressing P-glycoprotein (P-gp) by targeting MAP/ERK kinase kinase 1 (MEKK1). J Exp Clin Cancer Res 2016;35:25.
16. Liu N, Li J, Zhao Z, Han J, Jiang T, Chen Y, et al. MicroRNA-302a enhances 5-fluorouracil-induced cell death in human colon cancer cells. Oncol Rep 2017;37:631–9.
17. Wu Y, Hu L, Qin Z, Wang X. MicroRNA-302a upregulation mediates chemo-resistance in prostate cancer cells. Mol Med Rep 2019;19: 4433–40.
18. Chen P, Huang HP, Wang Y, Jin J, Long WG, Chen K, et al. Curcumin overcome primary gefitinib resistance in non-small-cell lung cancer cells through inducing autophagy-related cell death. J Exp Clin Cancer Res 2019;38:254.
19. Li L, Gong Y, Xu K, Chen W, Xia J, Cheng Z, et al. ZBTB28 induces autophagy by regulation of FIP200 and Bcl-XL facilitating cervical cancer cell apoptosis. J Exp Clin Cancer Res 2021;40:150.
20. Yu Z, Tang H, Chen S, Xie Y, Shi L, Xia S, et al. Exosomal LOC85009 inhibits docetaxel resistance in lung adenocarcinoma through regulating ATG5-induced autophagy. Drug Resistance Updates 2023; 67:100915.
21. Wang Z, Yang L, Wu P, Li X, Tang Y, Ou X, et al. The circROBO1/KLF5/FUS feedback loop regulates the liver metastasis of breast cancer by inhibiting the selective autophagy of afadin. Mol Cancer 2022; 21:29.
22. Hu F, Song D, Yan Y, Huang C, Shen C, Lan J, et al. IL-6 regulates autophagy and chemotherapy resistance by promoting BECN1 phosphorylation. Nat Commun 2021;12:3651.
23. Galluzzi L, Green DR. Autophagy-independent functions of the autophagy machinery. Cell 2019;177:1682–99.
24. Devis-Jauregui L, Eritja N, Davis ML, Matias-Guiu X, Llobet-Navàs D. Autophagy in the physiological endometrium and cancer. Autophagy 2021;17:1077–95.
25. Xiang H, Zhang J, Lin C, Zhang L, Liu B, Ouyang L. Targeting autophagy-related protein kinases for potential therapeutic purpose. Acta Pharm Sin B 2020;10:569–81.
26. Wang H, Tang Z, Liu S, Xie K, Zhang H. Acrylamide induces human chondrocyte cell death by initiating autophagy-dependent ferroptosis. Exp Ther Med 2023;25:246.
27. Charni-Natan M, Goldstein I. Protocol for primary mouse hepatocyte isolation. STAR Protoc 2020;1:100086.
28. Chen T, Bao S, Chen J, Zhang J, Wei H, Hu X, et al. Xiaojianzhong decoction attenuates aspirin-induced gastric mucosal injury via the PI3K/AKT/mTOR/ULK1 and AMPK/ULK1 pathways. Pharm Biol 2023;61:1234–48.
29. Han H, Yang C, Ma J, Zhang S, Zheng S, Ling R, et al. N^7-methylguanosine tRNA modification promotes esophageal squamous cell carcinoma tumorigenesis via the RPTOR/ULK1/autophagy axis. Nat Commun 2022;13:1478.
30. Zhu L, Wang J, Wu Z, Chen S, He Y, Jiang Y, et al. AFF4 regulates osteogenic potential of human periodontal ligament stem cells via mTOR-ULK1-autophagy axis. Cell Proliferation 2023;57:e13546.
31. Hashimoto Y, Yoshida Y, Yamada T, Aisu N, Yoshimatsu G, Yoshimura F, et al. Current status of therapeutic drug monitoring of 5-fluorouracil prodrugs. Anticancer Res 2020;40:4655–61.
32. Sethy C, Kundu CN. 5-fluorouracil (5-FU) resistance and the new strategy to enhance the sensitivity against cancer: implication of DNA repair inhibition. Biomed Pharmacother 2021;137:111285.
33. Sun Z, Shi K, Yang S, Liu J, Zhou Q, Wang G, et al. Effect of exosomal miRNA on cancer biology and clinical applications. Mol Cancer 2018; 17:147.

34. Shao P, Qu WK, Wang CY, Tian Y, Ye ML, Sun DG, et al. MicroRNA-205-5p regulates the chemotherapeutic resistance of hepatocellular carcinoma cells by targeting PTEN/JNK/ANXA3 pathway. Am J Transl Res 2017;9:4300–7.
35. Shi L, Wu L, Chen Z, Yang J, Chen X, Yu F, et al. MiR-141 activates Nrf2-dependent antioxidant pathway via down-regulating the expression of Keap1 conferring the resistance of hepatocellular carcinoma cells to 5-Fluorouracil. Cell Physiol Biochem 2015;35: 2333–48.
36. Guo M, Gan L, Si J, Zhang J, Liu Z, Zhao J, et al. Role of miR-302/367 cluster in human physiology and pathophysiology. Acta Biochim Biophys Sin 2020;52:791–800.
37. Lin SL, Ying SY. Mechanism and method for generating tumor-free iPS cells using intronic microRNA miR-302 induction. Methods Mol Biol 2018;1733:265–82.
38. Wang Y, Zhao L, Xiao Q, Jiang L, He M, Bai X, et al. miR-302a/b/c/d cooperatively inhibit BCRP expression to increase drug sensitivity in breast cancer cells. Gynecol Oncol 2016;141:592–601.
39. Qi Y, Qi W, Liu S, Sun L, Ding A, Yu G, et al. TSPAN9 suppresses the chemosensitivity of gastric cancer to 5-fluorouracil by promoting autophagy. Cancer Cell Int 2020;20:4.
40. Li YJ, Lei YH, Yao N, Wang CR, Hu N, Ye WC, et al. Autophagy and multidrug resistance in cancer. Chin J Cancer 2017;36:52.
41. Xu Z, Han X, Ou D, Liu T, Li Z, Jiang G, et al. Targeting PI3K/AKT/mTOR-mediated autophagy for tumor therapy. Appl Microbiol Biotechnol 2020;104:575–87.

Supplementary Material: This article contains supplementary material (https://doi.org/10.1515/oncologie-2023-0530).